ELSEVIER

Theoretical and Applied Fracture Mechanics 25 (1996) 73–81

theoretical and applied fracture mechanics

Fractal dimension evolution of microcrack net in disordered materials

A. Carpinteri [*,a], G.P. Yang [b]

[*,a] *Department of Structural Engineering, Politecnico di Torino, 10129 Torino, Italy*
[b] *Department of Civil Engineering, Tsinghua University, Beijing, P.R. China*

Abstract

Fractal geometry is used to evaluate the degree of disorder of crack size distribution in brittle damaging materials. The fractal dimension of the 2D microcrack net turns out to increase from one to two during the loading process and microcrack propagation. This means that the material becomes more disordered with the damage evolution. The longer cracks, in fact, propagate more rapidly than the shorter and, at the same time, the crack size distribution increases its statistical dispersion. Some numerical examples, related to different initial microcrack densities and size distributions, are illustrated with the computer simulation of the system evolution.

1. Introduction

As a new mathematical tool, Fractal Geometry [1,2] has been widely used for the description of irregular phenomena in various scientific fields recently. In the subjects concerning strength and fracture behavior of engineering materials, fractals represent the fracture surfaces in two or three-dimensional problems, just as for the original motivation to measure the length of irregular coastlines. Up to now, almost the whole research work on the fractal aspects in fracture mechanics of disordered materials has been concentrated on the evaluations of the fractal dimensions of fracture trajectories or surfaces. On the other hand, fractal geometry is not only useful to study complex shapes, but also it may be a powerful tool in describing damage phenomena with statistical characteristics. For example, in disordered materials like rocks, concrete and ceramics, there are many random parameters (i.e., position, size and orientation of the pre-existing microcracks). The microcracks propagate during the loading process and, at the same time, the parameters evolve with their statistical characters.

In this paper, Fractal concepts will be used to evaluate the evolving degree of disorder in the crack size distribution of the material. A fractal dimension measuring the microcrack size distribution is defined, and the variation of this parameter is continuously computed during the microcrack propagation process. It is found that the defined fractal dimension increases with the propagation of the cracks. In other words, it turns out that the materials become progres-

* Corresponding author. Fax +39 11 564 4899.

PII S0167-8442(96)00009-2

sively more disordered with the development of the crack net, from the initial loading to the failure stage.

2. Fractal description of crack size distribution

2.1. Initial fractal distribution

The cumulative probability of the existence of microcracks whose lengths are longer than a specific value a_1 is

$$P(a_1) = \int_{a_1}^{\infty} p(x)\,\mathrm{d}x, \tag{1}$$

where $p(x)$ is the probability density. Assume the form [3,4]:

$$p(x) = kNx^{-(N+1)} = kNx^{-(1/(D-1))}, \tag{2}$$

where k is a constant, and $D = (N+2)/(N+1)$. It follows that

$$P(a_1) = \int_{a_1}^{\infty} kNx^{-(N+1)}\,\mathrm{d}x = k\left[-x^{-N}\right]_{a_1}^{\infty} = ka_1^{-N}. \tag{3}$$

With the cumulative distribution given by the above power law, the crack size distribution appears as a kind of fractal distribution with exponent N:

$$N = \frac{\mathrm{Log}\ P(a_1) - \mathrm{Log}\ k}{\mathrm{Log}(1/a_1)}. \tag{4}$$

N is only a measure of the degree of order in crack size distribution [5]. Alternatively, we can define $D = (N+2)/(N+1)$ as the fractal dimension of the crack size distribution in the specimen, so that the variation range of this fractal dimension is between 1 and 2, when N takes positive values as shown in Fig. 1. Larger values of N correspond to more ordered situations such that it can be referred to as the "Order Parameter".

If the total number of cracks in specimen is n_t, and a_1 is any specific crack length, then

$$n_{a \geq a_1} + n_{a < a_1} = n_t \tag{5}$$

and

$$n_{a \geq a_1} = n_t - n_{a < a_1} = ka_1^{-N} = ka_1^{-(2-D)/(D-1)}, \tag{6}$$

where

$$D = 1 + \frac{\mathrm{Log}\ a_1}{\mathrm{Log}\ a_1 + \mathrm{Log}\ k - \mathrm{Log}\ n_{a \geq a_1}}. \tag{7}$$

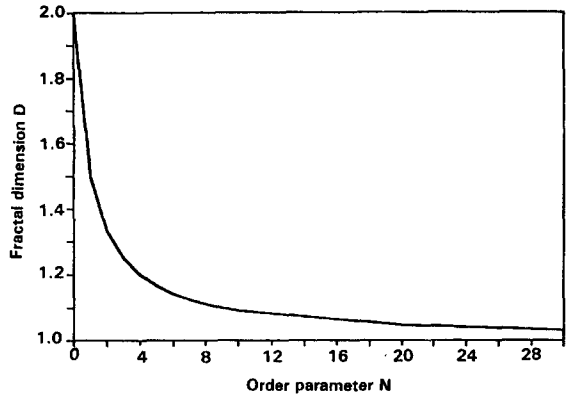

Fig. 1. Fractal dimension D versus order parameter N.

According to the above definition, when $D = 1$, N tends to infinity and we have the ideal ordered material, as well as, when $D = 1.5$, $N = 1$ corresponds to the self-similarity defined in [5], and the material turns out to be very disordered.

If the total number of cracks n_t, the minimum and maximum lengths of cracks, $a_{\min}$ and $a_{\max}$, and the initial fractal dimension D_0 are given as initial conditions, then from

$$n_t = k\left(\frac{1}{a_{\min}^N} - \frac{1}{a_{\max}^N}\right) \tag{8}$$

the constant k, corresponding to the given fractal crack size distribution, can be evaluated.

For a given initial crack configuration, actual crack size a_i is obtained from the following estimation:

$$k\left(\frac{1}{a_{\min}^N} - \frac{1}{a_i^N}\right) = i \quad (i = 1, 2, \ldots, n_t). \tag{9}$$

When i ranges from 1 to n_t, all the crack lengths $a_1, a_2, \ldots, a_{n_t}$ are obtained.

For the sake of simplicity, uniform distributions are adopted for crack position and orientation.

2.2. Fractal parameter evolution with propagating cracks

The major objective of this paper is to study the evolution of the fractal parameter corresponding to different degrees of disorder in crack size distribution during microcrack propagation. In the computer

simulation, the total load is provided by different step increments. At each step, the number of cracks whose length is longer than a given characteristic value a_1 is computed and the value of fractal dimension is determined from Eq. (7).

The evaluation of the total crack length during propagation is based on the assumption that the length of an initial crack with branching is effectively equal to the summation of the lengths of the branching cracks and that of the initial crack. This assumption is valid for both cases of prevailing tension and prevailing compression.

From a theoretical point of view, fractal dimension D should be the same for any reference crack length a_1, if the distribution is exactly a fractal one. However, since only a finite number of cracks and finite crack lengths could be simulated, the average value is taken over three evaluations connected with different crack lengths a_1:

$$a_1 = \frac{a_{\max} + a_{\min}}{4}, \quad \frac{a_{\max} + a_{\min}}{2}, \quad \frac{3(a_{\max} + a_{\min})}{4}. \tag{10}$$

In this way, three different fractal dimensions are obtained and the average value related to a specific loading level is considered.

3. Crack propagation model

In the case of mixed mode fracture and many random cracks, when computing the Stress Intensity Factors (SIFs), it is convenient to use the fictitious stress on the crack surfaces even though the crack surfaces are stress-free. In other words, only the on-site conditions for each crack are considered for obtaining the SIFs [6].

3.1. Specimen in tension

For the sake of simplicity, the stress field generated by a single microcrack is simulated with the same one corresponding to a crack in an infinite elastic solid. Suppose that there is only a preexisting crack of length a_i in mixed mode loading condition as shown in Fig. 2. The SIFs at its tips are assumed to be K_{I} and K_{II}, respectively.

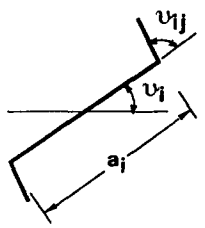

Fig. 2. Inclined crack.

From the well-known maximum hoop stress criterion, the crack tip j ($j = 1, 2$) will begin propagating when

$$\cos\frac{\theta_{ij}}{2}\left[K_{\mathrm{I}} \cos^2\frac{\theta_{ij}}{2} - \tfrac{3}{2}K_{\mathrm{II}} \sin\theta_{ij}\right] = K_{\mathrm{IC}} \tag{11}$$

where K_{IC} is the Mode I fracture toughness of the material, and the propagation angle θ_{ij}, which is the value corresponding to the tip j of the crack i, satisfies the condition

$$K_{\mathrm{I}} \sin\theta_{ij} + K_{\mathrm{II}}(3\cos\theta_{ij} - 1) = 0. \tag{12}$$

Now, if the original crack of length a_i has propagated with two branching cracks b_i, as shown in Fig. 3, the fictitious stresses σ and τ on the surfaces of the original crack, generated by the remote applied loads, result in an opening force O and a sliding force S on the branching cracks.

In the case of different orientations of random cracks, the normal stress σ may be positive or negative with consideration of different lateral stresses, although the major stress is tensile:

$$O = \begin{cases} a_i(-\tau \sin\theta_{ij} + \sigma \cos\theta_{ij}), \\ \quad \text{for} \quad \sigma > 0, \\ a_i(-\tau \sin\theta_{ij} + \sigma\lambda|\sin\theta_{ij}|), \\ \quad \text{for} \quad \sigma < 0, \end{cases} \tag{13a}$$

$$S = a_i(\tau + \sigma\lambda)\cos\theta_{ij}, \tag{13b}$$

where λ is the friction coefficient between the two crack surfaces in compression. When the normal stress is positive, the frictional term in Eq. (13b) is absent.

For the computation of the SIFs at each tip of the branching crack, an analogous problem, where an

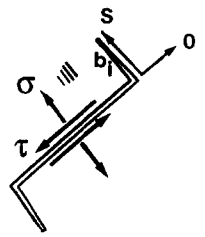

Fig. 3. Branching cracks.

opening force P and a sliding force Q act on a crack surface (Fig. 4), has to be considered:

$$K_{\mathrm{I}}^{\mathrm{A}} = \frac{1}{2\sqrt{\pi a}}\left[P\sqrt{\frac{a+b}{a-b}} + Q\left(\frac{c-1}{c+1}\right)\right], \tag{14a}$$

$$K_{\mathrm{II}}^{\mathrm{A}} = \frac{-1}{2\sqrt{\pi a}}\left[P\left(\frac{c-1}{c+1}\right) - Q\sqrt{\frac{a+b}{a-b}}\right]. \tag{14b}$$

The constant c depends on the material properties and the stress state in the specimen. In the case of a pair of forces, and specially for the problem shown in Fig. 3, together with the roles of remote vertical stress σ_1 and lateral stress σ_2 applied on the boundary of the specimen, the SIFs at each tip of the branching crack are evaluated from

$$K_{\mathrm{I}} = \frac{O}{\sqrt{\pi b_i}} + \sqrt{\pi b_i}\left[\frac{\sigma_1+\sigma_2}{2} + \frac{\sigma_1-\sigma_2}{2}\cos 2(\theta_i+\theta_{ij})\right], \tag{15a}$$

$$K_{\mathrm{II}} = \frac{S}{\sqrt{\pi b_i}} + \sqrt{\pi b_i}\left[\frac{\sigma_1-\sigma_2}{2}\sin 2(\theta_i+\theta_{ij})\right]. \tag{15b}$$

In the case of random cracks, the normal stress in the bracket of Eq. (15a) may be positive or negative depending on possible lateral stress. If the fictitious

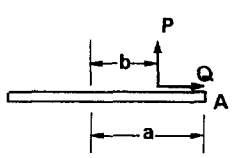

Fig. 4. Problem analogous to that of Fig. 3.

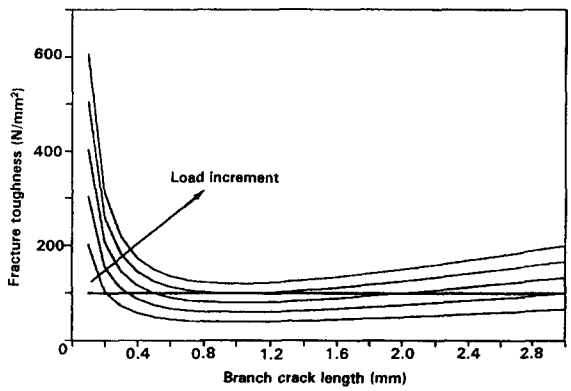

Fig. 5. Variation of the crack length solutions.

normal stress on the branching cracks is positive, the propagation length b_i should be determined from

$$\frac{a_i(-\tau\sin\theta_{ij} + \sigma\cos\theta_{ij})}{\sqrt{\pi b_i}} + \sqrt{\pi b_i}\left[\frac{\sigma_1+\sigma_2}{2} + \frac{\sigma_1-\sigma_2}{2}\cos 2(\theta_i+\theta_{ij})\right] = K_{\mathrm{IC}}. \tag{16}$$

The solution of Eq. (16) can be expressed in compact form:

$$(A/x) + Bx = K_{\mathrm{IC}}, \tag{17}$$

where $x = \sqrt{\pi b_i}$ $(x \geq 0)$. The solution can be obtained by the intersections of the curve and the straight line in Fig. 5. It can be seen from Fig. 5 that there may be three different situations for the solution of the branching crack.

If the values of A and B satisfy the condition

$$4AB < K_{\mathrm{IC}}^2 \tag{18}$$

the length of the branching crack presents two positive roots. The smaller should be taken as the true solution since the branching crack propagates progressively from zero to a relatively stable value, for which a small increment of the length will cause decrease of the SIFs.

The values of A and B increase with the increment of the applied loads, and the propagation length of the branching crack will increase progressively. The critical condition will occur when $4AB = K_{\mathrm{IC}}^2$ (only one intersection exists).

The propagation of the branching crack will become unstable if $4AB > K_{\mathrm{IC}}^2$ (there is no intersection in this case).

It can be demonstrated that there is a relatively stable stage of microcrack propagation in brittle specimen even under prevailing tension, if the external stresses are not too high.

3.2. Specimen in compression

The effective stresses σ, τ on the surfaces of the original crack of length a_i result in an opening force

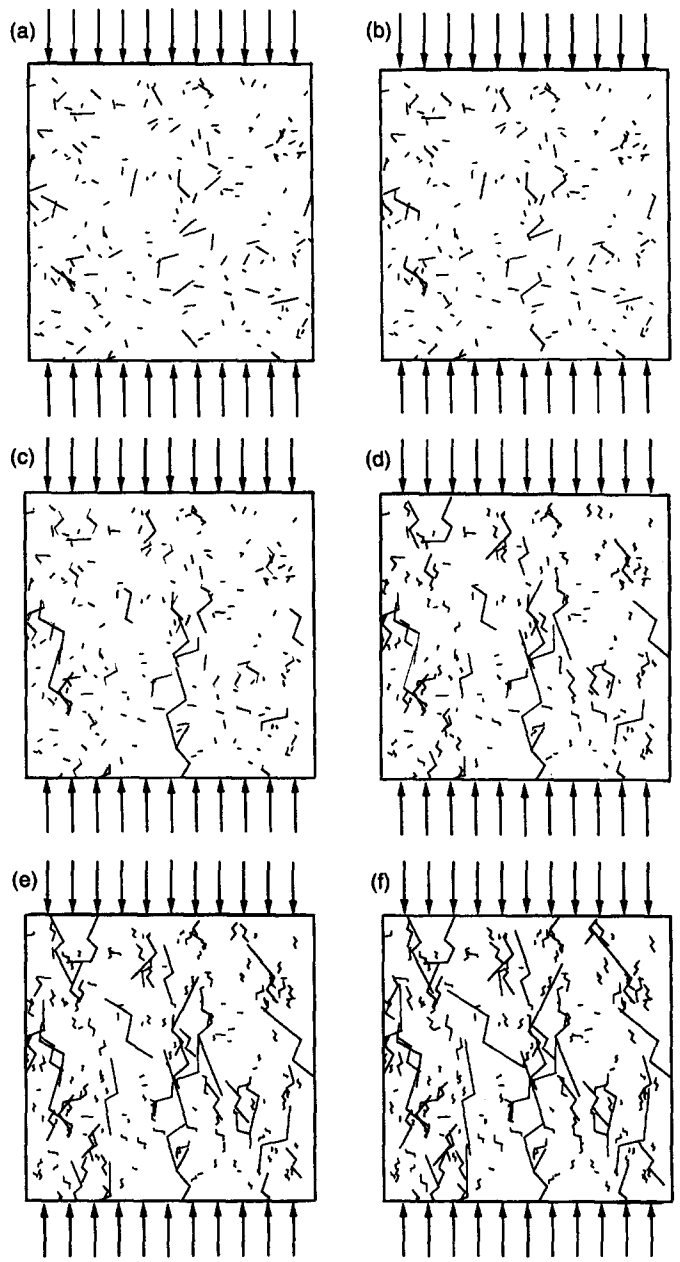

Fig. 6. (a) Initial microcrack distribution. (b) Microcrack pattern at the second loading step. (c) Microcrack pattern at the fourth loading step. (d) Microcrack pattern at the sixth loading step. (e) Microcrack pattern at the eighth loading step. (f) Microcrack pattern at the final stage.

O and a sliding force S on the branching cracks of length b_i (Fig. 3). When the remote stress is compressive, the normal stress σ is negative (compressive) in most cases:

$$O = a_i\left(-\tau \sin \theta_{ij} + \sigma\lambda \left| \sin \theta_{ij} \right|\right), \tag{19a}$$

$$S = \begin{cases} a_i(\tau + \sigma\lambda) \cos \theta_{ij}, & \text{for } \tau > 0, \\ a_i(\tau - \sigma\lambda) \cos \theta_{ij}, & \text{for } \tau < 0. \end{cases} \tag{19b}$$

If the normal stress on the original crack is positive, then there is no resistant friction force.

Considering the randomness in the distribution of crack orientation and lateral stress, the normal stress may be also positive or negative. If it is positive, the propagation length can be obtained step by step from Eq. (16).

If the normal stress is negative, then from

$$\frac{a_i\left(-\tau \sin \theta_{ij} + \sigma\lambda \left| \sin \theta_{ij} \right|\right)}{\sqrt{\pi b_i}} = K_{IC} \tag{20}$$

we know that the propagation of the branching crack is stable, so its length can be obtained step by step with the increase of the applied external stresses on the specimen.

4. Examples

Some examples are shown to study the evolution of the fractal dimension of the microcrack distribution during the propagation process, from the initial loading to the failure stage. These examples include different crack numbers and different initial fractal dimensions. The results always show that the fractal dimension increases with the development of the microcrack net, i.e. the materials become more disordered with the damage evolution. Although this paper is only an initial attempt to study the evolution of the microcrack fractal dimension during the material damage process, the results are reasonable from the physical point of view since the longer cracks propagate more rapidly than the shorter, so that the microcrack size distribution becomes more disperse.

During crack propagation, some branching cracks may intersect with other primary or branching cracks. The assumption that the branching crack will stop propagating is adopted in the case of intersection. From the comparisons between different crack patterns obtained from arrest or non-arrest intersection crack assumptions, it is found that the results with arrest are more realistic (see Section 4.2). According to the "arrest model", if two branching cracks intersect, they both will arrest. On the other hand, in the case that a primary crack meets a branching crack, only the branching crack arrests, whereas the primary can propagate through the branching.

4.1. Evolution of the fractal dimension of the microcrack net

The first example deals with a square specimen of side 100 mm containing 200 microcracks with initial fractal dimension 1.40. The minimum initial crack length is 1 mm and the maximum is 10 mm. In each loading step, a stress increment of -40 N/mm^2 is applied. The original crack distribution and the subsequent crack patterns up to failure are shown in Figs. 6a to 6f. The variation of the fractal dimension concerning the crack size distribution is shown in Fig. 7, where the fractal dimension increases with the development of the microcrack net during the material damage process. This means that the material becomes more disordered when damaged.

4.2. Comparison between different crack intersection models

From the experimental observation, it is found that some intersection cracks do arrest propagating

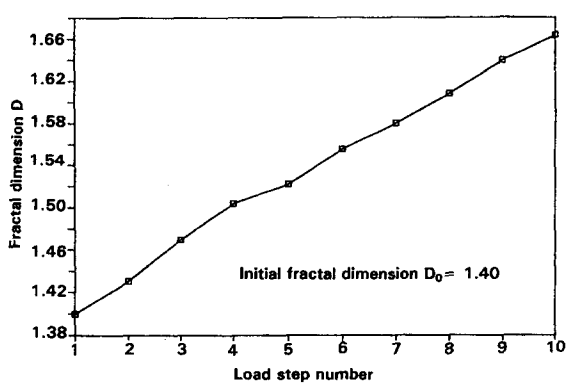

Fig. 7. Evolution of the fractal dimension during microcrack propagation.

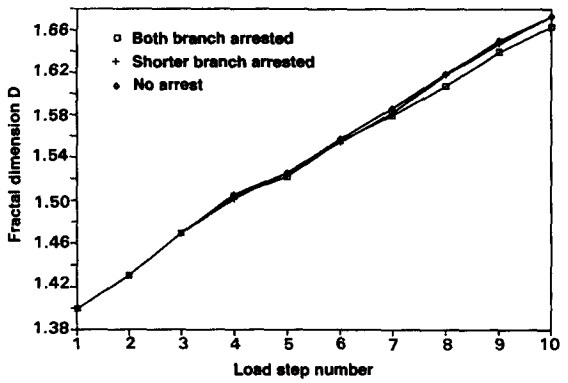

Fig. 8. Results with different crack arresting assumptions.

while, in other cases, some intersection cracks do not. To evaluate the effects of the different models for the intersection crack arrest behavior on the variation of the fractal dimension, three different situations are considered. The first assumption is that intersection does not affect propagation so that branching cracks and primary cracks can pass across each other without arrest. The second assumption is that only the shorter branching crack arrests whereas the longer propagates. The last assumption is that both branching cracks will arrest at the same loading stage as mentioned in the preceding section. The evolution of the fractal dimension with these three different assumptions is shown in Fig. 8, from which it is found that, although the fractal dimension corresponding to no-arrest is a little greater than those of the other cases, there are no remarkable differences between the three different assumptions.

The crack patterns at the final stage, with the shorter branching crack arrest and both non-arresting cracks are shown in Figs. 9a and 9b, respectively. These two figures can be compared with Fig. 6f, in which both cracks arrest. It appears that the assumption of both arresting cracks is a little more reasonable from usual experimental experience, so that such assumption is adopted in all the remaining examples.

4.3. Results from different initial fractal dimensions

With the same crack number and the same initial minimum and maximum crack lengths, different initial fractal dimensions provide different crack size

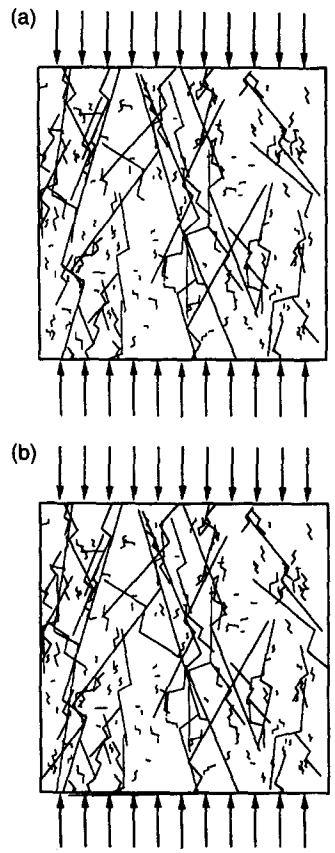

Fig. 9. (a) Microcrack pattern at the final stage with the assumption of arresting shorter branching cracks. (b) Microcrack pattern at the final stage with the assumption of non-arresting cracks.

distributions in the specimen. The third example is about the evolution of the different initial fractal dimensions during the material damage process. The

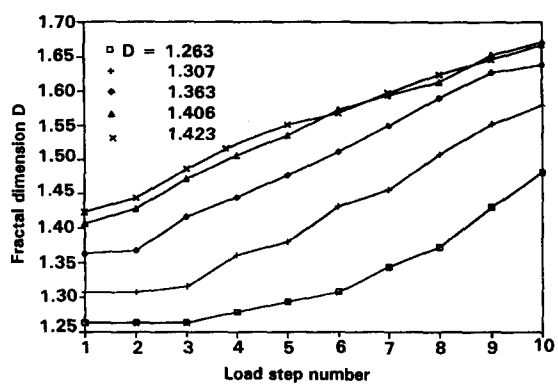

Fig. 10. Fractal dimension evolutions from different initial values.

Table 1
Fractal dimensions and differences

Initial	1.263	1.307	1.363	1.406	1.423
Final	1.481	1.580	1.639	1.671	1.667
Difference	0.218	0.273	0.276	0.265	0.244

crack number is 100 and the initial minimum and maximum crack lengths are again 1 mm and 10 mm, respectively. Five initial fractal dimensions are considered ranging from 1.263 to 1.423 (a stress increment of -40 N/mm^2 in each loading step is applied). Their evolutions are shown in Fig. 10, while the differences between the initial and final values are shown in Table 1. From Fig. 10 and Table 1 it can be seen that the variation ranges of the dimensions from the initial to the final stage are between 0.218 and 0.276.

4.4. Results with different confining stresses

With the aim of studying the evolution of the fractal parameter during microcrack propagation with different confining stresses, the specimen with 200 cracks is loaded by a compression of -40 N/mm^2 at each loading step, while five different lateral stresses, equal to -8, -4, 0, $+2$, $+4$ N/mm^2, are applied. The results are shown in Fig. 11, in which the specimen failed at the fourth loading step with lateral tensile stress of $+4$ N/mm^2. From Fig. 11 it can be found that the increment of the fractal dimension is more rapid when there is a greater lateral tension. Very different crack patterns with lateral ratios of -0.1 and $+0.2$ are shown in Figs. 12a and 12b, respectively.

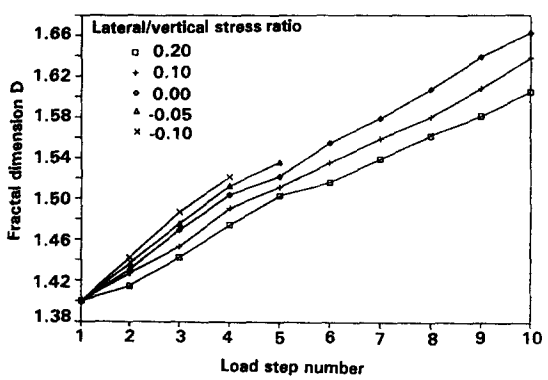

Fig. 11. Fractal dimension evolutions with different lateral stresses.

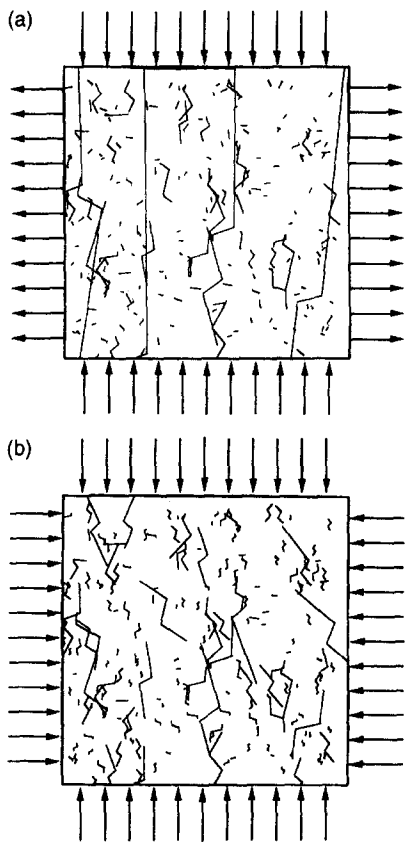

Fig. 12. (a) Microcrack pattern at final stage with lateral tension equal to 4 N/mm^2. (b) Microcrack pattern at final stage with lateral compression equal to -8 N/mm^2.

5. Concluding remarks

As an attempt to describe the irregularities of crack size in brittle materials, a statistical fractal dimension is defined to evaluate the disorder degree in crack size distribution. It appears that this parameter can represent the complex damage process of the material during crack propagation.

The evolution of the fractal dimension is continuously computed during the microcrack propagation process to study the fracture behavior of disordered materials in the loading process. Some examples with different influence parameters are shown. The

results always show that the fractal dimension increases with the development of the microcrack net. It means that the materials become more disordered with the damage evolution.

References

[1] B.B. Mandelbrot, *The Fractal Geometry of Nature* (Freeman and Company, New York, 1982).

[2] K. Falconer, *Fractal Geometry: Mathematical Foundations and Applications* (Wiley & Sons, Chichester, 1990).

[3] A. Carpinteri, *Mechanical Damage and Crack Growth in Concrete: Plastic Collapse to Brittle Fracture* (Martinus Nijhoff, Dordrecht, 1986).

[4] A. Carpinteri, Decrease of apparent tensile and bending strength with specimen size: two different explanations based on fracture mechanics, *Int. J. of Solids and Structures* 25, 407–429 (1989).

[5] A. Carpinteri, Scaling laws and renormalization groups for strength and toughness of disordered materials, *Int. J. of Solids and Structures* 31, 291–302 (1994).

[6] Guo-ping Yang and Xila Liu, Interaction and propagation of random microcracks in compression, *Studi e Ricerche*, Politecnico di Milano, Italy, 14, 121–141 (1993).